Supporting Information

Controlled Synthesis of Near-infrared Quantum Dots for Optoelectronic Devices

Hui Zhang,[1] Gurpreet S. Selopal,[1,2] Yufeng Zhou,[1] Xin Tong, [1,2] Daniele Benetti,[1] Lei Jin,[1] Fabiola Navarro-Pardo,[1,2] Zhiming Wang,[2] Shuhui Sun,[1,2] Haiguang Zhao,[1]* Federico Rosei[1,2]*

[1] Institut National de la Recherche Scientifique, 1650 Boulevard Lionel-Boulet Varennes, Quebec J3X 1S2, Canada

[2] Institute of Fundamental and Frontier Science, University of Electronic Science and Technology of China, Chengdu 610054, People's Republic of China

1. Synthesis of QDs

1.1 Synthesis procedures of lead precursors in literature[1]

Synthesis of lead oleate from lead oxide: typically, lead oxide (PbO) (10.00 g, 44.8 mmol) and acetonitrile (20 mL) are added to 100 mL round bottom flask. The suspension is stirred while being cooled in an ice bath for five minutes. Then trifluoroacetic acid (0.7 mL, 8.96 mmol) and trifluoroacetic anhydride (6.2 mL, 44.8 mmol) were added to the same flask. After the yellow lead oxide dissolved, the solution became clear and colorless (labelled solution A). Oleic acid (25.437 g, 90.05 mmol), isopropanol (180 mL) and thiethylamine (10.246 g, 101.25 mmol) were added to 500 mL flask (labelled solution B). Solution A was added to solution B with stirring, resulting in the formation of a white precipitate. A clear and colorless solution was obtained after the mixture was heated for 10 min. Then the heat was switched off and the flask was slowly cooled down to room temperature, following further cooling in a -20 °C freezer overnight. The resulting white powder was isolated by suction filtration, and then dried under vacuum for 12 h. Finally the white powder was stored in a nitrogen filled glove box.

1.2 Preparation of the TGA-capped water-soluble QDs

The as-prepared oil-soluble QDs were transferred to water using the ligand exchange method, following other reports.[2] Specifically, 0.13 mL TGA was added to 1.0 mL methanol. The pH of solution was adjusted to 8 with 30% NaOH, then was injected into the 5 mL of oil-soluble QDs and stirred for 10 min. Subsequently 15 mL of deionized water was added into the solution and stirred for 5 min at room temperature. The solution was separated into two phases and QDs were distributed in the upper layer of water in the reaction solution. The water soluble QDs were precipitated by adding acetone and then re-dispersed in pH=9 deionized water with 30% NaOH.

2. Fabrication of QDSSCs sensitized by water-soluble QDs

TiO_2/QDs anode preparation is performed with the dip method. Specifically, TGA-capped water-soluble QDs were deposited on the mesoporous TiO_2 film by dropping 40 μL water-soluble QDs solution on a mesoporous TiO_2 film and then stored in a refrigerator (4 °C) for 3 h. Following rinsing in water and ethanol, the photoanodes were treated and QDSSCs were assembled in the same way as described in the experimental section.

3. Figures and Tables

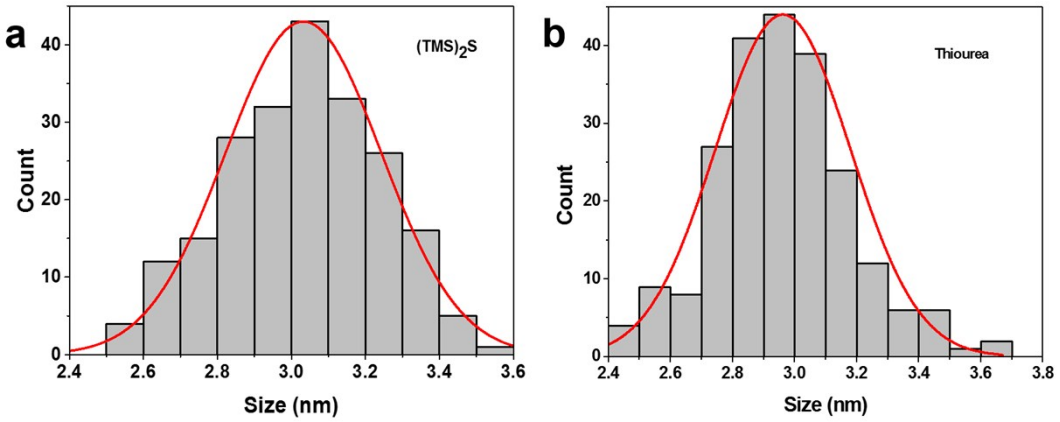

Figure S1 The size distribution of colloidal Cd-PbS QDs from [$(TMS)_2S$] (a) and thiourea (b). Red lines show the fitting results. Sizes are measured from more than 200 QDs in the TEM images respectively.

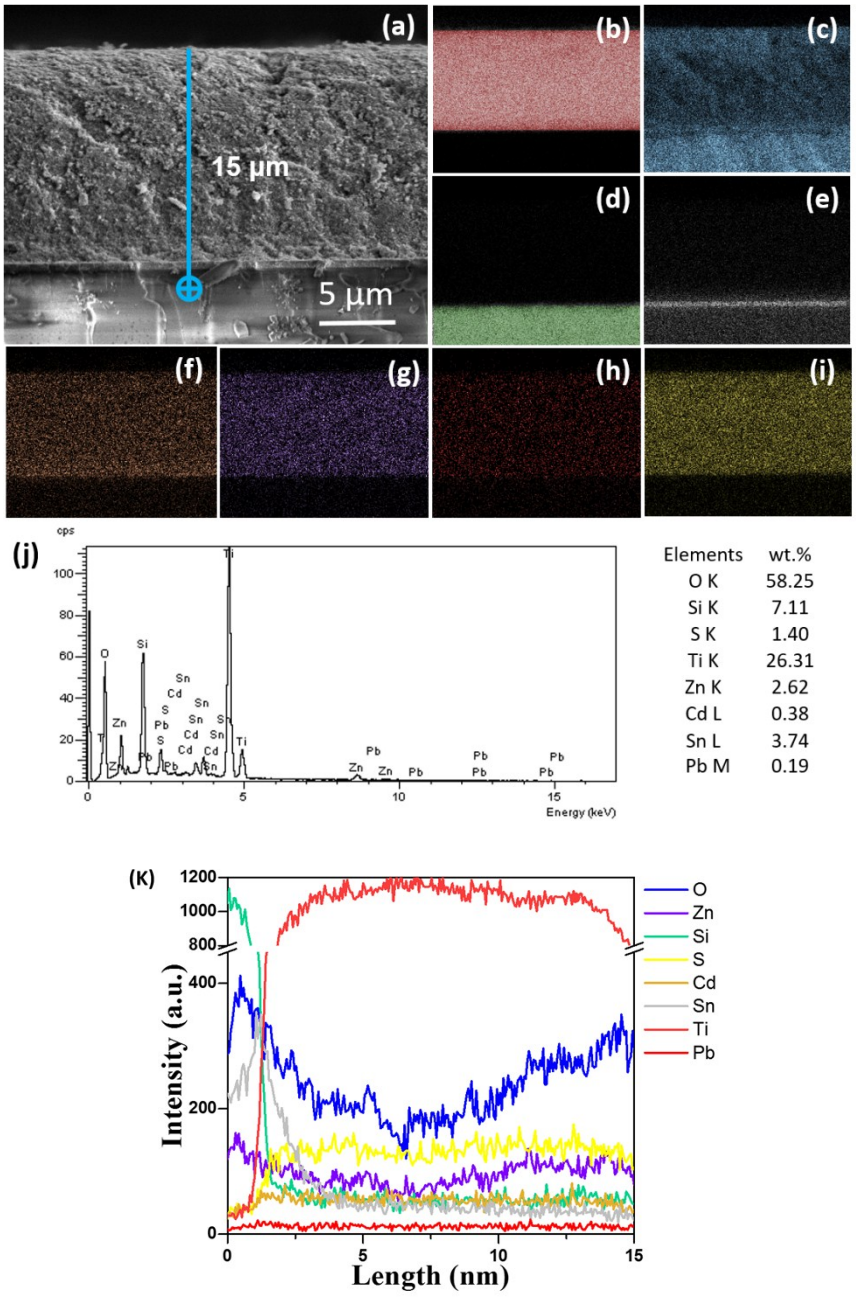

Figure S2 (a) Representative SEM cross-sectional image of TiO_2/QDs photoanode capped with ZnS, (b-i) EDS 2D mapping: the elements distribution of Ti (b), O(c), Si(d), Sn(e), Cd(f), Zn(g), Pb(h) and S(i); (j) EDS spectra; (k) EDS line mapping.

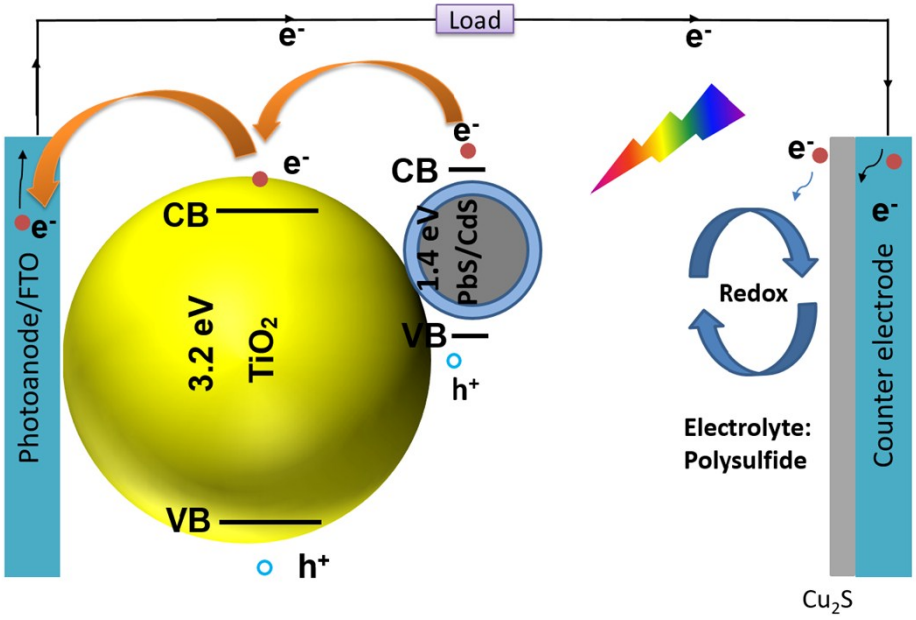

Figure S3 Schematic illustration of QDSSCs with the prepared QDs as sensitizer for photoanode and Cu_2S as the counter electrode.

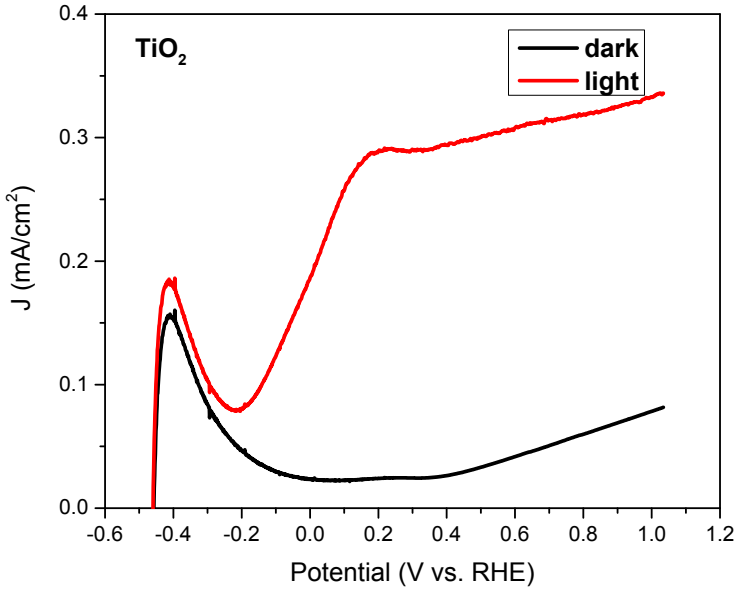

Figure S4 Photocurrent density versus the applied voltage (vs RHE) curves of PEC devices assembled using bare TiO_2 under one simulated sunlight illumination (AM 1.5 G, 100 $mW \cdot cm^{-2}$) in the dark (black line) and constant one sunlight illumination (red line).

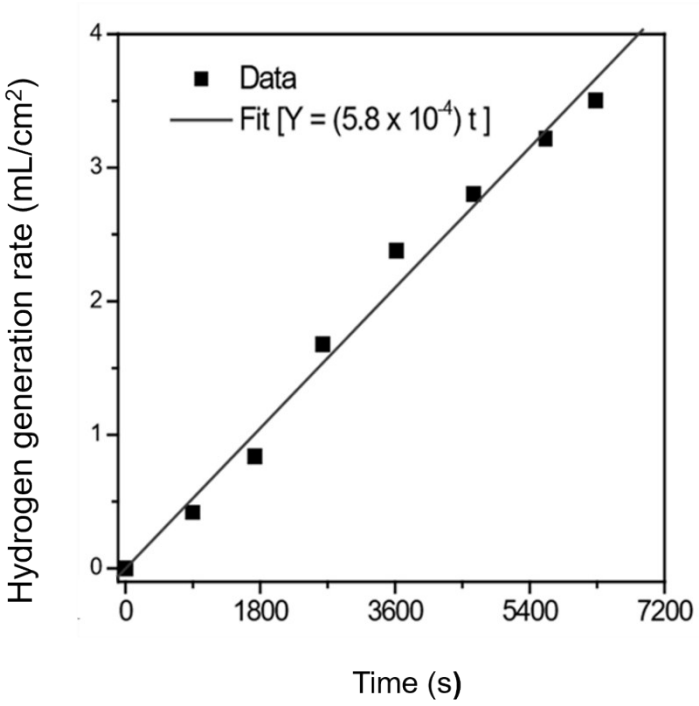

Figure S5 H_2 evolution of CdSe/CdS QDs, as a function of time at 0.2 V vs. RHE under 100 mW/cm^2 illumination with AM 1.5 G filter. The evolution of H_2 exhibits a nearly linear increase over time. Current density is around 6.5 mA/cm^2 at 0.2 V vs. RHE under 100 mW/cm^2 illumination with AM 1.5 G filter. The preparation of CdSe/CdS sensitized TiO_2 anode was following ref 3.

We measured H_2 with gas chromatography on the CdSe/CdS QD system using the CdSe/CdS QDs sensitized anode and Pt counter electrode to monitor the H_2 evolution as a function of time as this type of QD is more stable compared to PbS QDs and presents a very accurate trend between the current density and time. Based on the calibration curve, we calculated the hydrogen generation rate in the similar PEC system (only QDs are not same type). Based on the reference curve, we integrate the current density (Figure 4c) and the calculated hydrogen generation rate is around 0.50 mL·cm^{-2}·h^{-1} (equal to 12 mL·cm^{-2}·day^{-1}) in the anode based on QDs synthesised via thiourea. This is higher than that of 0.38 mL·cm^{-2}·h^{-1} (equal to 9.1 mL·cm^{-2}·day^{-1}) obtained from the anode based on QDs synthesised via [$(TMS)_2S$].

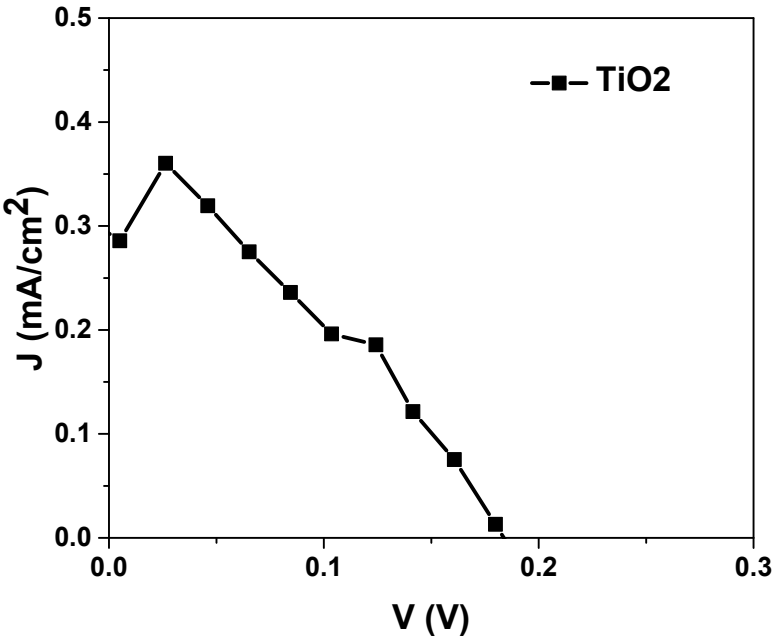

Figure S6 *J–V* curves of devices with only TiO_2 as photo-harvester under one simulated sunlight.

The *J-V* curves of QDSSCs sensitized by bare TiO_2 are shown in Figure S6. The device yields a J_{sc} of 0.293 mA/cm^2, V_{oc} of 0.184 V, FF of 0.427 and PCE of 0.023%.

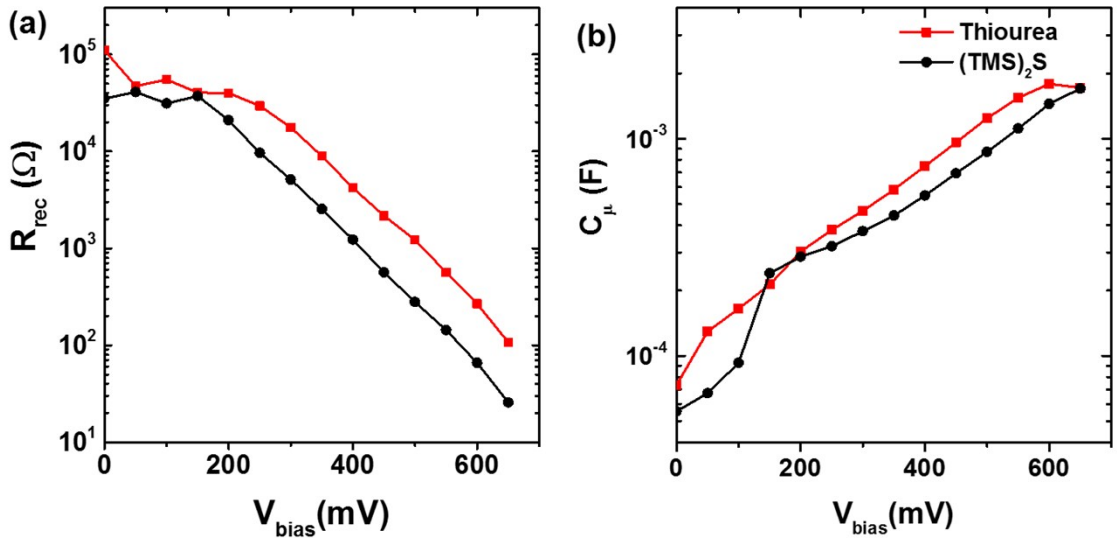

Figure S7 Electrochemical impedance spectroscopy of representative samples of devices sensitized with QDs from thiourea and $(TMS)_2S$. (a) Recombination resistance, (b) Chemical Capacitance.

EIS characterization was performed to further understand the charge recombination and transport for devices sensitized with QDs from thiourea and [$(TMS)_2S$]. The recombination resistance (R_{rec}) takes into account recombination phenomena occurring at the photoanode/electrolyte interfaces.[4, 5] Figure S7a shows the dependence of R_{rec} on the forward bias applied to the devices. For the whole range of V_{bias}, the values of R_{rec} for the devices sensitized with QDs from thiourea are higher than those made with QDs from [$(TMS)_2S$]. Since R_{rec} is inversely proportional to the charge recombination rate, the significantly higher value of R_{rec} for devices sensitized with QDs from thiourea implies that the charge recombination rate is significantly suppressed, boosting the injection of electrons in the photoanode. This observation is in good agreement with the device's functional performance (as shown in table 1). The chemical capacitance (C_μ) stands for the variation of electron density dependent on the Fermi level and monitors the distribution of trap states in the band gap of the TiO_2 matrix.[4] As shown in Figure S7b, similar C_μ values of both devices are observed, indicating that the different QDs sensitizers do not affect the CB edge position of TiO_2.[5-7]

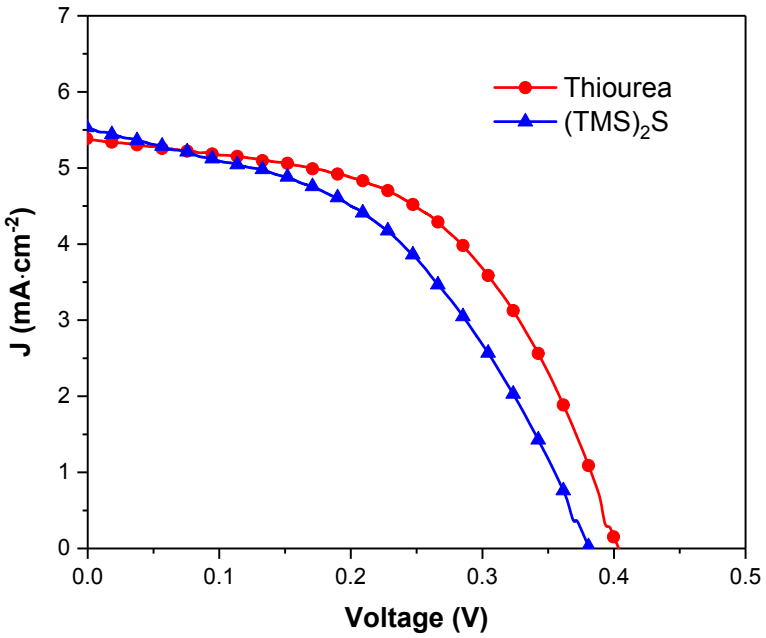

Figure S8 *J–V* curves of QDSSCs which sensitized by prepared QDs with similar overall size of 3.2 nm and shell thickness of 0.2 nm from different sulphur precursor under one simulated sunlight.

Table S1 Functional performances of QDSSCs sensitized with PbS QDs from different sulphur precursor.

QDs from different sulphur precursor	**Absorbance peak (nm)**	**Size (nm)**	**Cd-treatment PbS Core/CdS shell thickness (nm)**	**J_{sc} (mA/cm²)**	**V_{oc} (V)**	**FF**	**PCE (%)**
[$(TMS)_2S$]	996	3.2	3.0/0.2	5.50 (±0.10)	0.38 (±0.07)	0.46 (±0.08)	0.96 (±0.06)
Thiourea	980	3.2	3.0/0.2	5.35 (±0.12)	0.40 (±0.05)	0.53 (±0.05)	1.14 (±0.08)

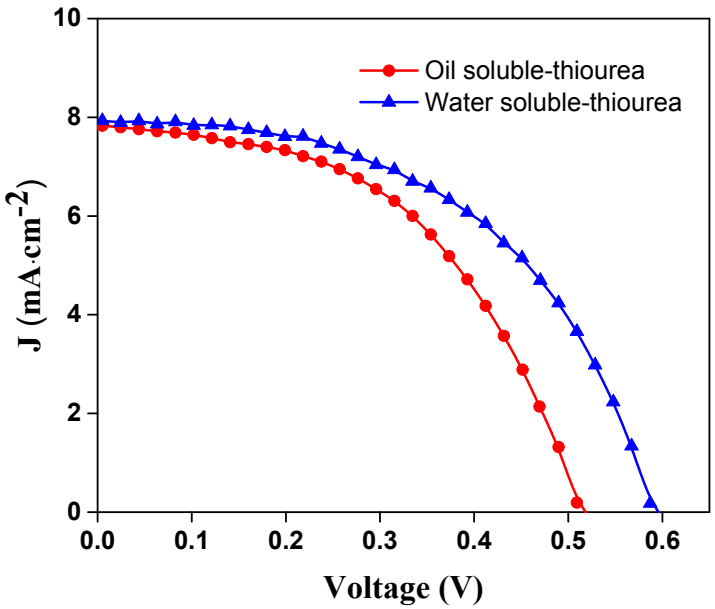

Figure S9 *J–V* curves of QDSSCs which sensitized by prepared oil soluble and water soluble QDs from sulphur precursor of thiourea under one simulated sunlight.

Table S2 Functional performances of QDSSCs sensitized with oil soluble and water soluble QDs from sulphur precursor of thiourea.

Different kind of QDs	J_{sc} (mA/cm²)	V_{oc} (V)	FF	PCE (%)
Oil-soluble	7.84 (±0.16)	0.52 (±0.01)	0.49 (±0.03)	2.00 (±0.06)
Water-soluble	10.72 (±0.04)	0.55 (±0.06)	0.50 (±0.03)	2.95 (±0.03)

References

1 M. P. Hendricks, M. P. Campos, G. T. Cleveland, I. Jen-La Plante, J. S. Owen, *Science*, 2015, **348**, 1226-1230.

2 S. Jiao, J. Wang, Q. Shen, Y. Li and X. Zhong, *J. Mater. Chem. A*, 2016, **4**, 7214–7221.

3 R. Adhikari, L. Jin, F. Navarro Pardo, D. Benetti, B. AlOtaibi, S. Vanka, H. Zhao, Z. Mi, A. Vomiero and F. Rosei, *Nano Energy*, 2016, **27**, 265.

4 I. Mora-Seró, S. Giménez, F. Fabregat-Santiago, R. Gómez, Q. Shen, T. Toyoda and J. Bisquert, *Acc. Chem. Res.*, 2009, **42**, 1848-1857.

5 V. González-Pedro, X. Xu, I. Mora-Seró and J. Bisquert, *ACS Nano*, 2010, **4**, 5783-5790.

6 J. Du, Z. Du, J.-S. Hu, Z. Pan, Q. Shen, J. Sun, D. Long, H. Dong, L. Sun, X. Zhong and L.-J. Wan, *J. Am. Chem. Soc.*, 2016, **138**, 4201-4209.

7 Z. Pan, I. Mora-Seró, Q. Shen, H. Zhang, Y. Li, K. Zhao, J. Wang, X. Zhong and J. Bisquert, *J. Am. Chem. Soc.*, 2014, **136**, 9203-9210.